

## CEBAF Cryomodule Commissioning in the South Linac

M. Drury, H. Lankford, T. Lee, J. Marshall, J. Preble, Q. Saulter, W. Schneider, M. Spata, M. Wiseman  
 Continuous Electron Beam Accelerator Facility  
 12000 Jefferson Ave, Newport News, VA 23606-1909

### Abstract

When complete, the Continuous Electron Beam Accelerator Facility will house a 4 GeV recirculating linear accelerator containing 42 1/4 cryomodules arrayed in two antiparallel linacs and an injector. Currently, 38 1/4 cryomodules have been installed. Each cryomodule contains eight superconducting niobium 5-cell rf cavities that operate at 1.497 GHz [1]. A cryomodule must provide an energy gain of 20 MeV to the 200 $\mu$ A beam [2]. The resultant dynamic heat load must be less than 45 W. The cavity parameters that are measured during the commissioning process include the external Q's ( $Q_{ext}$ ) of the cavity ports, the unloaded Q ( $Q_o$ ) of the cavity as a function of accelerating gradient, and the maximum operating gradient of the cavity [3]. Finally, the mechanical tuners are cycled and characterized. A portable test stand allows local control of the rf system and provides automated data acquisition. During the period from April 1993 through September 1993, 16 of the 20 cryomodules installed in the South Linac were commissioned. All cryomodules tested in the South Linac meet or exceed the CEBAF specifications. This paper describes the results of the commissioning of the first 10 cryomodules in the South Linac.

### Introduction

Each cryomodule is commissioned after installation to determine whether it meets the requirements necessary for proper operation of the accelerator. A detailed set of calorimetric measurements is made of cavity  $Q_o$  vs.  $E_{acc}$  characteristics. During this process, the frequencies of the cavity fundamentals ( $f_o$ ), the  $Q_{ext}$ 's of the fundamental power couplers, and the external Q's of the field probes ( $Q_{fp}$ ) are also measured. Careful logging of interlock faults, quenches, measurement of radiation, and analysis of  $Q_o$  degradation are used to determine the maximum usable gradient ( $E_{max}$ ) for each cavity. The CEBAF Design Handbook specifies the requirements for each of the cavity rf characteristics. These specifications are shown in Table 1.

Table 1 Cavity Parameters

$Q_{ext}$	(fundamental power coupler)	$6.6 \times 10^6 \pm 20\%$
$Q_{fp}$	(field probe)	$1.3 \times 10^{11} \begin{matrix} +62\% \\ -37\% \end{matrix}$
$Q_o$		$\geq 2.4 \times 10^9$
$f_o$	( $\pi$ mode, T=2K)	1.497 GHz
$E_{max}$		$\geq 5.0$ MV/m
Pressure Sensitivity		$< 60$ Hz/torr

The cryomodule production group has put together a portable test stand that is controlled by a Macintosh computer. This system allows fully interlocked local control of the rf system. Using this system, the commissioning of a cryomodule can be completed in about three eight hour shifts. The system includes a voltage controlled oscillator for klystron drive, a spectrum analyzer, several power meters, a frequency counter, and a heater controller for the cryomodule internal heaters. The Macintosh controls the test sequence and provides automated data collection, and real-time analysis of the data. Geiger-Mueller tubes are installed on the beam line axis at either end of the cryomodule, and at the points where the waveguides enter the cryomodule to monitor radiation from field emission.

### Results

Figure 1 shows the distribution of measurements for  $Q_{ext}$ . About half of the cavities have  $Q_{ext}$  values at or below the lower limit of the specification. The  $Q_{ext}$ 's of the fundamental power couplers are all measured prior to installation and adjusted where necessary. It has become apparent, however that connecting the cavity to the waveguide system in the tunnel has an adverse effect on the value of  $Q_{ext}$ . This is probably due to mismatches in the system. In most cases,  $Q_{ext}$  is lower once

connected to the waveguide system. Since the lowered  $Q_{ext}$ 's do not seriously effect machine operation, no attempts have yet been made to rectify the situation.

Figure 2 shows the distribution of measurements of  $Q_{fp}$ . Most of these measurements fall into the range specified by the Design Handbook. There are a few however, that fall well outside the specified range. The field probes that have  $Q_{fp}$ 's above  $2.1 \times 10^{11}$  are likely the result of contamination in the connection between the cryomodule and the external cable. In many cases, the connectors have been found to be contaminated with moisture or other chemical residues that cause electrical shorts in the connector and degrade the rf signal from the field probe. Use of contact cleaners and heat guns have relieved the problem in all cases. Some of the dirty connectors were not discovered until high power testing had commenced.

Figure 3 illustrates the distribution of cavity  $Q_0$ 's at 5 MV/m (the operating gradient for the accelerator). All but two of the cavities tested have exceeded the design requirements. The two that did not meet specification have suffered degradation due to an unknown agency. These cavities are currently undergoing detailed testing in order to determine the cause or causes of the  $Q_0$  degradation [4].

Maximum usable gradient is defined by a number of factors. It is defined by the commissioning team as 90 % of quench gradient, 90 % of the gradient at which interlock faults prohibit sustained operation, or the gradient at which field emission loading reaches 1 Watt. Cavities are also prohibited from operating beyond a gradient at which measured radiation from field emission reaches 1 R/hr. Obviously, if more than one of these conditions apply to a cavity, the lowest gradient limit is chosen. The interlock faults include waveguide arcs, waveguide and beam line vacuum, and warm window temperature. Most of the cavities in the South Linac have maximum gradients limited by field emission loading. Figure 4 shows the current distribution of maximum usable gradients in the South Linac. Two of the cavities are listed as having an  $E_{max}$  of 0.0 MV/m. These are the same cavities mentioned above that have  $Q_0$ 's that do not meet specification. Currently, it has been decided not to operate these cavities. The other cavities in these cryomodules will easily make up the energy deficit. It should be noted that the cryomodules containing these cavities are still able to meet the 20 MeV and dynamic heat load requirements.

Figures 6 and 7 illustrate the radiation levels measured at  $E_{max}$ . These levels are determined in most cases by the field emission loading limit. This is evident from an examination of Figures 8 and 9 which show the maximum radiation levels recorded. It should be noted that the VCO drive is interlocked to shut down when measurable radiation reaches 2 R./hr.

## Conclusion

Cryomodule performance in the South Linac continues to exceed CEBAF design requirements. These 10 cryomodules together are capable of producing 287 MV of gradient with a dynamic heat load of 420 W. The major limiting factor on maximum gradient is now field emission loading.

## References

- [1] P. Kneisel, et al, "Performance of Superconducting Cavities for CEBAF", *Conference Record of the 1991 IEEE Particle Accelerator Conference* Vol. 4 pp. 2384-86
- [2] H. A. Grunder, et al, "The Continuous Electron Beam Accelerating Facility", *Proceedings of the 1987 IEEE Particle Accelerator Conference* Vol. 1 pp. 13-18
- [3] M. Drury, et al, "Commissioning of the CEBAF Cryomodule ", *Proceedings of the 1993 IEEE Particle Accelerator Conference*
- [4] W. Schneider, et al "Anomalous  $Q_0$  Results in the South Linac," *contributed this conference.*

This work was supported by DOE contract DE-AC05-84ER40150



Distribution of Qext Measurements  
(Fundamental Power Coupler)

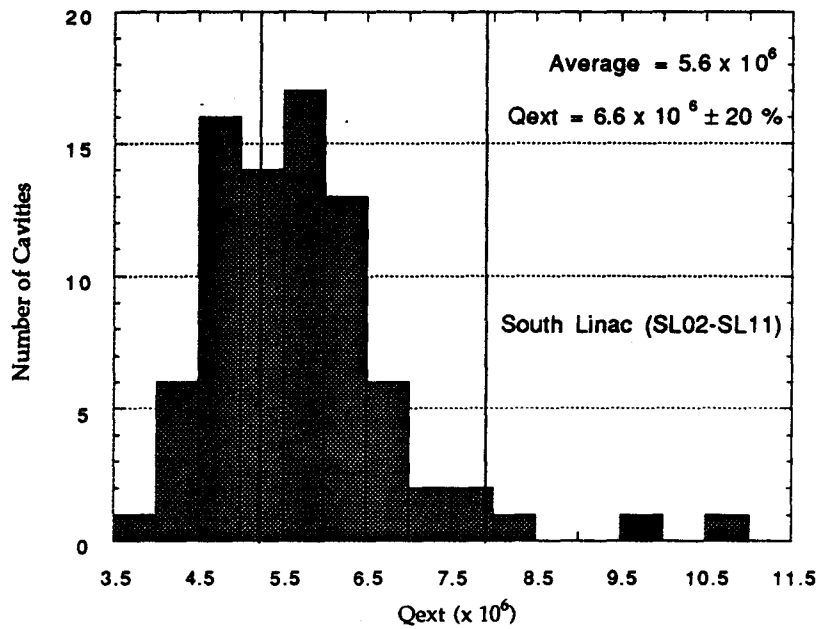


Figure 1



Distribution of Qext Measurements  
(Field Probe)

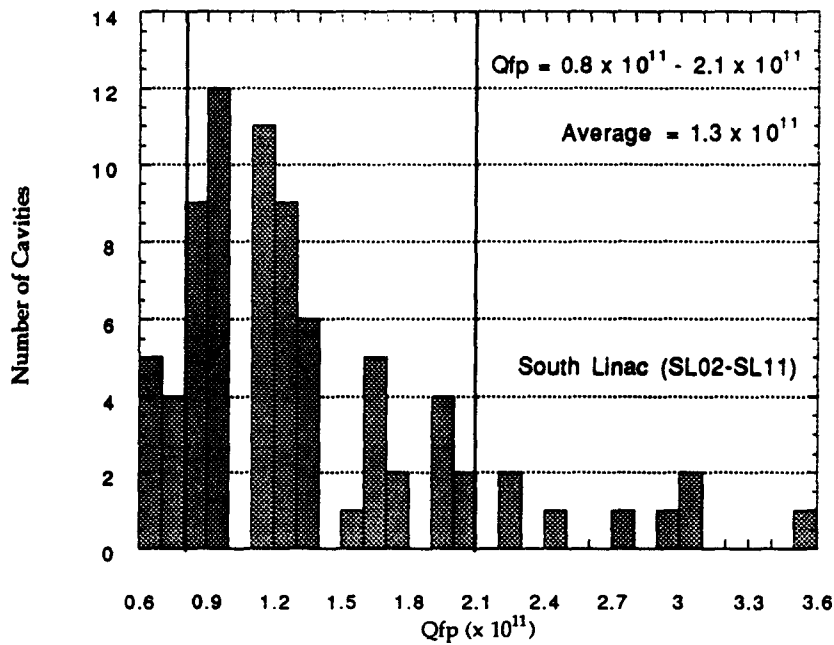


Figure 2



### Qo Distribution for S. Linac

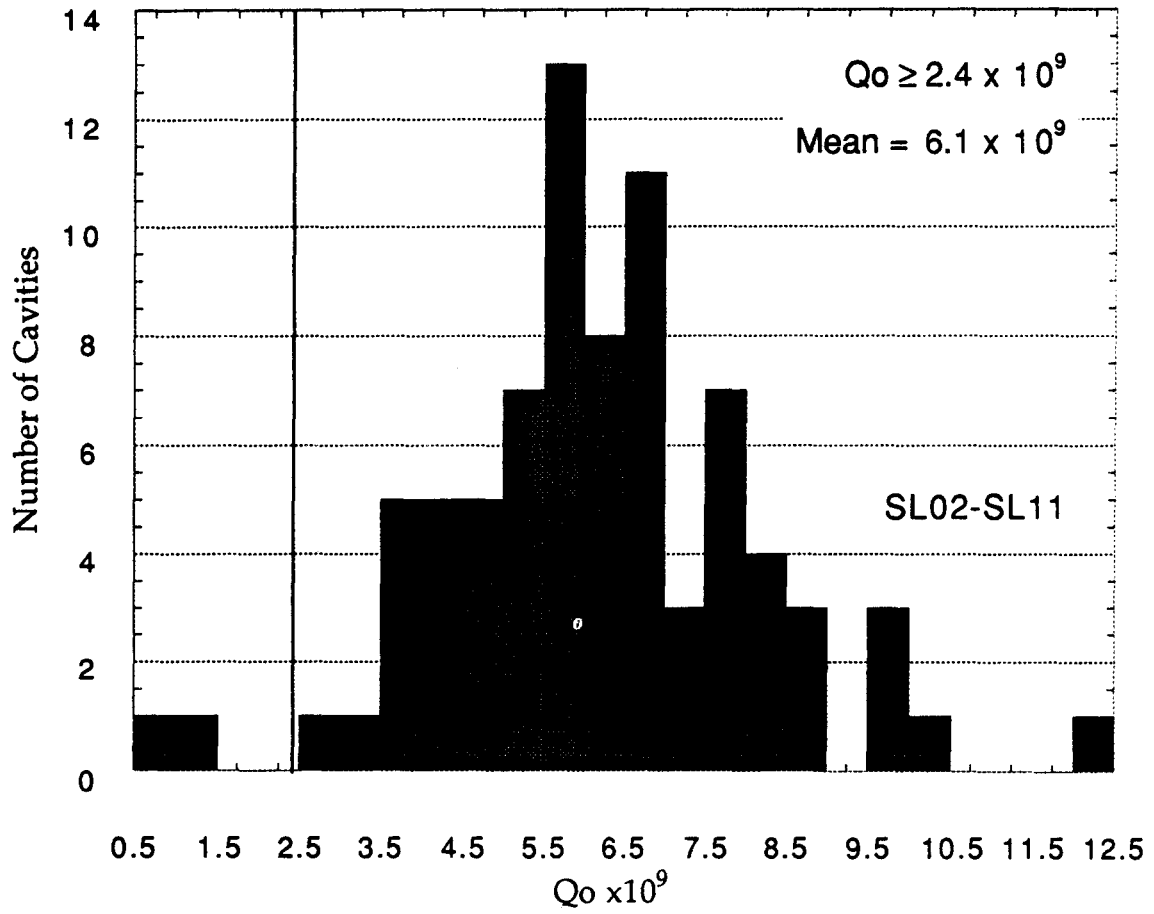


Figure 3

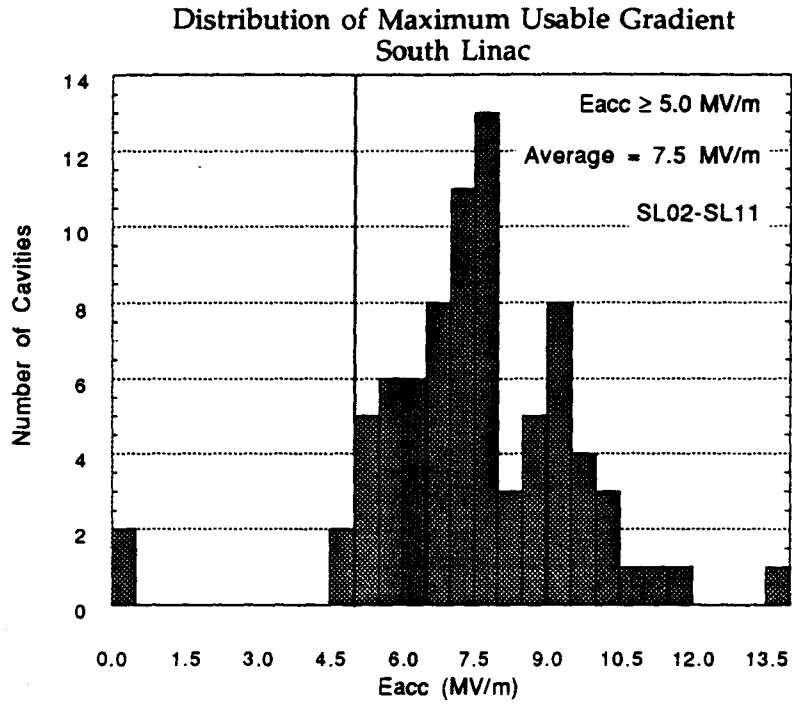


Figure 4

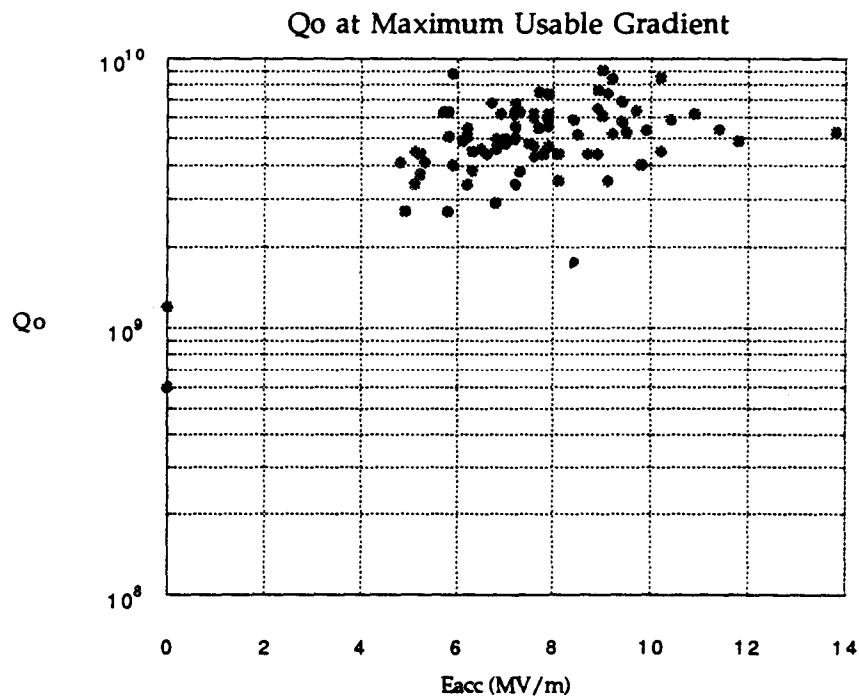
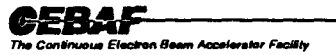


Figure 5

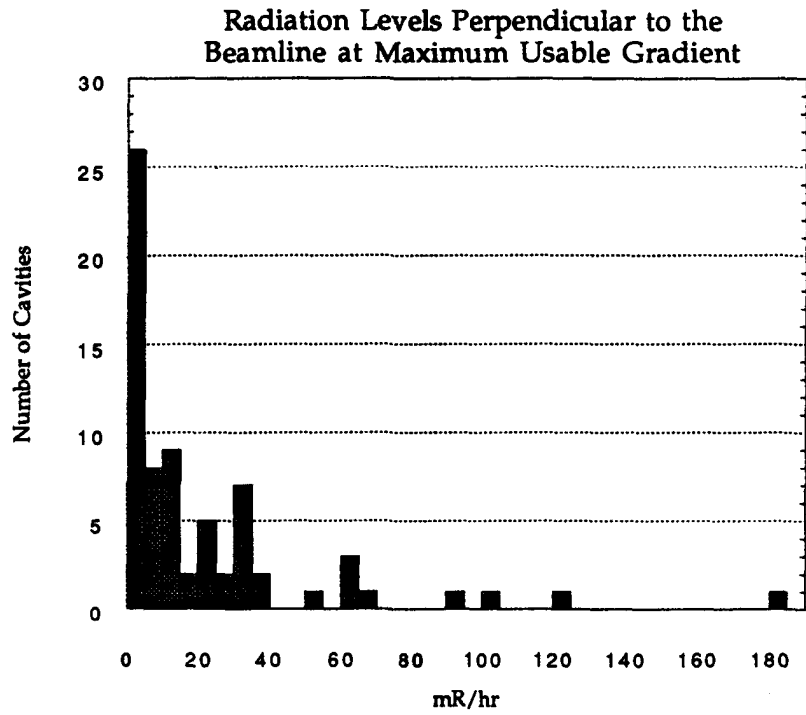


Figure 6

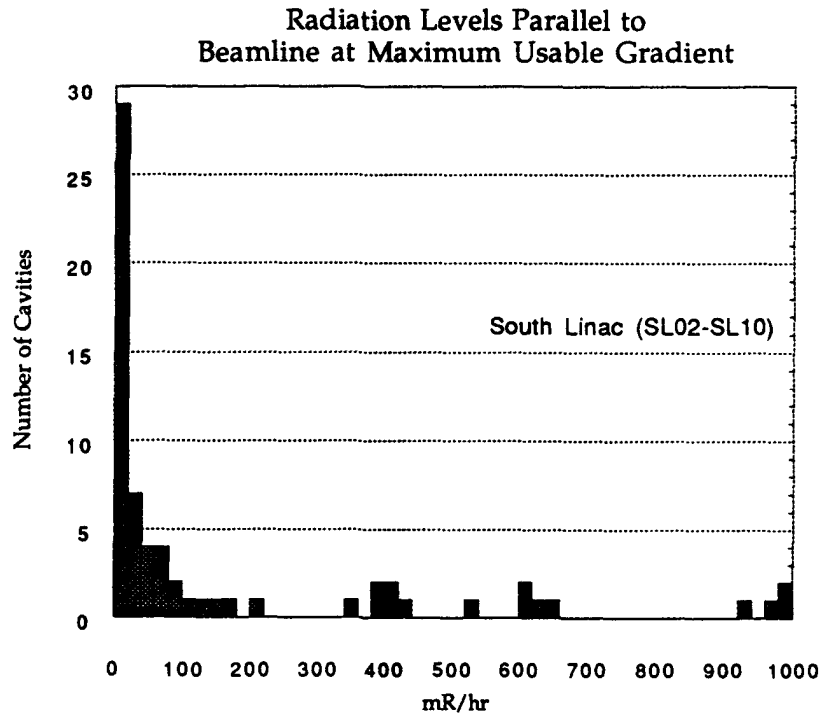


Figure 7

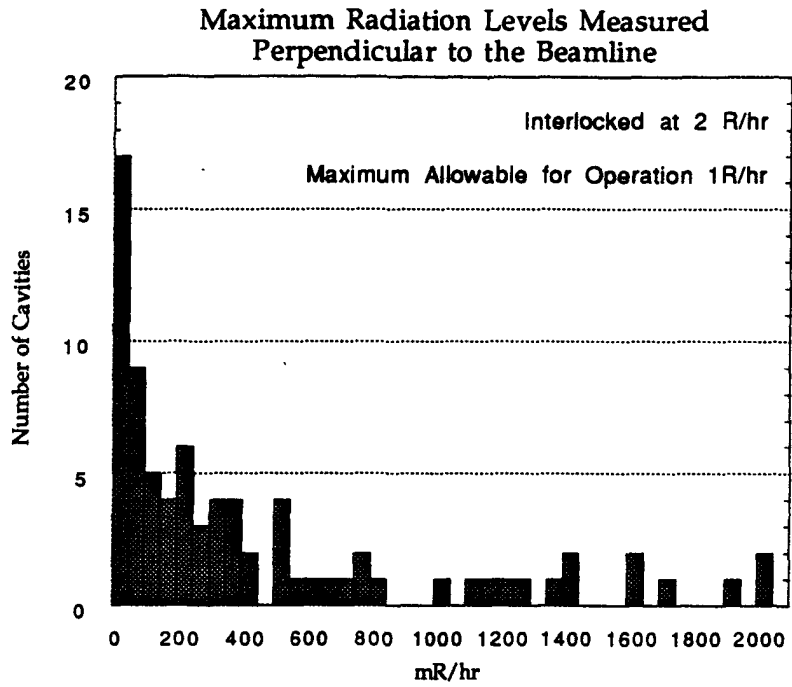


Figure 8

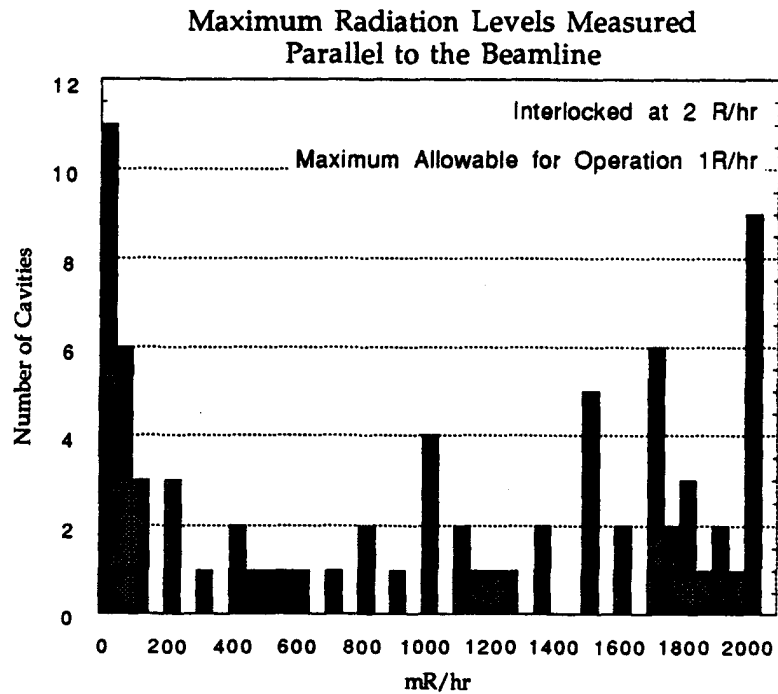


Figure 9